

УДК 539.1.07

## LIQUID ARGON POLLUTION TESTS OF THE ATLAS DETECTOR MATERIALS AT IBR-2 REACTOR IN DUBNA

*C. Leroy<sup>1</sup>, Yu. Borzunov, A. Cheplakov<sup>2</sup>, V. Chumakov, V. Golikov,  
L. Golovanov, S. Golubyh, V. Kukhtin, E. Kulagin, V. Luschikov,  
V. Minashkin, A. Shalyugin, A. Tsvinev*

A cold test facility has been in operation since October 1998 at the IBR-2 reactor of JINR, Dubna. During four measurement campaigns, various samples of the ATLAS forward (FCAL) and hadronic end-cap (HEC) calorimeter materials have been exposed to a fast neutron ( $E_n \geq 100$  keV) fluence of about  $10^{16}$  cm<sup>-2</sup>. The samples were immersed in a liquid argon cryostat, and an  $\alpha$  cell has been used as purity monitor. Results of the liquid argon pollution study obtained during these measurement campaigns are presented.

The investigation has been performed at the Laboratory of Particle Physics, JINR

### Проверка загрязнения жидкого аргона материалами детектора ATLAS на реакторе ИБР-2

*К. Леруа и др.*

С октября 1998 года на реакторе ИБР-2 действует облучательная установка для холодного тестирования материалов, на которой в течение четырех измерительных циклов облучались быстрыми нейтронами различные образцы материалов для адронного и форвард-калориметров детектора ATLAS до полного флюенса  $10^{16}$  см<sup>-2</sup>. При этом образцы материалов находились в криостате с жидким аргоном. В работе подробно изложены результаты исследования загрязнения жидкого аргона.

Работа выполнена в Лаборатории физики частиц ОИЯИ.

#### 1. DESCRIPTION OF THE FACILITY

General characteristics of the beam-line and details about dosimetry measurements performed at the IBR-2 reactor can be found in paper [1].

---

<sup>1</sup>Université de Montréal, Montréal (Québec) H3C 3J7, Canada  
e-mail: *leroy@LPS.U.Montreal.CA*

<sup>2</sup>e-mail: *cheplako@sunse.jinr.ru*

The cold test facility has been installed on both sides of a 6 m long shielding movable platform. The facility includes a cryostat which is filled with liquid argon. The cryostat containing test samples of materials is mounted on the support frame at the head of the platform. It can be brought into the irradiation zone through the hole of 80 cm diameter secured in the outer shielding wall of the reactor. Additional tubes in the platform have been used for cryogenic lines, signal cables as well as for transportation of another samples of materials for their irradiation. The dewar of liquid nitrogen for persistent feeding of the cryostat is also mounted on the rails behind the platform together with the control panel. The data taking equipment is assembled in the counting room located  $\sim 20$  m from the irradiation zone.

**1.1. Cryogenic System.** The main cryogenic scheme of our experiment is shown in Fig. 1. The facility provides the liquefaction of the gaseous argon in the argon vessel of the cryostat by means of liquid nitrogen and maintains a constant level of liquid argon during the whole period of irradiation. It includes the cryostat (1), the receiver of gaseous argon (2), the dewar filled with liquid nitrogen for persistent feeding of the cryostat (3), the piping for liquid nitrogen feeding to the cryostat (4) and the automatic system for maintaining the constant level of liquid argon (5).

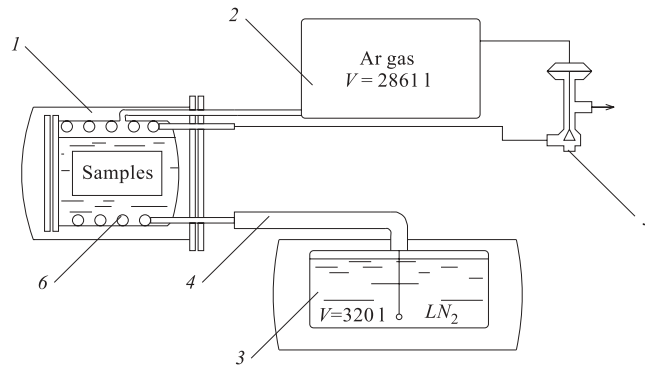


Fig. 1. Main cryogenic scheme of the facility: (1) cryostat, (2) receiver of gaseous argon, (3) dewar for liquid nitrogen, (4) liquid nitrogen piping, (5) automatic regulator, (6) argon condenser

The samples of materials to be tested have been placed inside the argon vessel of the cryostat. Its volume is about 1 litre. For stable operation, the occupancy of more than 50% of the vessel volume by the samples is not recommended. The argon condenser (6), the coil with the liquid nitrogen flow through it, is located inside the vessel. The vessel communicates with the receiver of 286 litres volume. The maximal pressure in the receiver of 2.5 bar is determined by the strength of the receiver and the cryostat. In total, 715 litres of argon gas is enough to fill the vessel with liquid argon up to 90% of its volume.

The liquid nitrogen for argon liquefaction is feeding the cryostat from the standard dewar of 320 litres volume via a special piping (4) of 17 m length. The nitrogen in the dewar has to be kept at the equilibrium state at the pressure of 1.8 bar. At lower pressure of liquid nitrogen, argon ice could be formed on the condenser walls, with the result of argon liquefaction slowing down and an increase of liquid nitrogen rate. The condensation temperature of argon is  $T_K = 87.5$  K at 1.05 bar and the vaporization temperature of nitrogen is  $T_V = 83.0$  K at 1.8 bar. Thus, the facility is operating in the temperature interval  $\Delta T = 4.5$  K.

The nitrogen rate regulator (5) provides a liquid argon constant level in the cryostat, automatically. The argon pressure in the vessel and receiver is the same. Deviation of the liquid argon level in the cryostat causes a pressure variation in the receiver. The pressure influences the regulator in such a way that it opens if the pressure is growing (in this case the argon liquefaction is going on due to a higher rate of liquid nitrogen, and the pressure falls) and vice versa. An analogous system was used successfully in the HYPOM experiment at Saclay [4].

Together with the argon pressure amplifier, this system allows one to keep the pressure of argon constant within  $\pm 0.05$  bar. The level of liquid argon remains stable within  $\pm 1$  mm. The system is autonomous: it only utilizes compressed gas (air) with a pressure of 1.4 bar at the rate of 3 l/hour. The «pneumatic nitrogen system» based on nitrogen gasification may be used as another gas source.

The rate of liquid nitrogen is determined by heat input to the nitrogen dewar, to the liquid nitrogen piping, and to the cryostat. The latter one consists of the heat generation from the environment and the heat release induced by the irradiation of the test samples and of the inner argon vessel. The heat input to the cryostat is estimated to be equal to 25 W. It is about 17 W for the nitrogen dewar and is equal to 34 W for the nitrogen piping. The total heat generation is about 76 W, that corresponds to the liquid nitrogen rate of  $(2.5 \div 3)$  l/hour. It takes about 15 minutes to cool off the argon vessel and 30 minutes to fill the vessel with liquid argon.

**1.2. Purification System for the Argon Gas.** The system to purify the argon gas was developed at the Bochvar Institute for Inorganic Materials in Moscow.

The metal hydrides method (IMC) [2] is the most effective to achieve high purification. The method is based on chemical reactions between gaseous impurities and metals or intermetallic compounds (IMC) which cause the formation of corresponding oxides, nitrites, carbides and hydrides. It allows the development of effective getters for molecular impurities and achieving a high performance gas purification technology.

The materials based on IMC can be also used for hydrogen accumulation. This technology can be applied for nitrogen and hydrogen purification from the chemical active gaseous impurities. For all specified gases, the impurities content in pure gas can be reduced to a level below 0.1 ppm.

The purification system produced for our experiment allows the removal of  $O_2$ ,  $N_2$ ,  $CH_4$ ,  $CO$ ,  $CO_2$ ,  $H_2O$  impurities. The system includes a vessel of 20 mm diameter and 300 mm length filled with IMC powder and a heater. The powder must be heated up to the temperature of 650–700 °C before use. The system has been successfully tested [3]. It was applied to purify the argon gas which contained 5000 ppm of nitrogen, 700 ppm of oxygen, and 900 ppm of water. The total content of impurities in the purified gas was found to be below the detection limit of 1 ppm.

The volume fraction of the standard argon gas used for radiation tests is about 99.998% before purification and total impurities amount to about  $(2 \div 5)$  ppm of  $O_2$ -equivalent. So, one may expect that the purity of the argon gas prepared for liquefaction in our experiment is better than the 1 ppm level.

**1.3. Electronics.** The main diagram of the electronics set-up is presented in Fig. 2. The CAMAC electronics is operated «on-line» by a personal computer.

High voltage of  $(0 \div +2)$  kV is applied to the anode of the  $\alpha$  cell. An  $^{241}\text{Am}$   $\alpha$ -source with an activity of 7.7 kBq/ $4\pi$  is deposited on the cathode and used for the electron

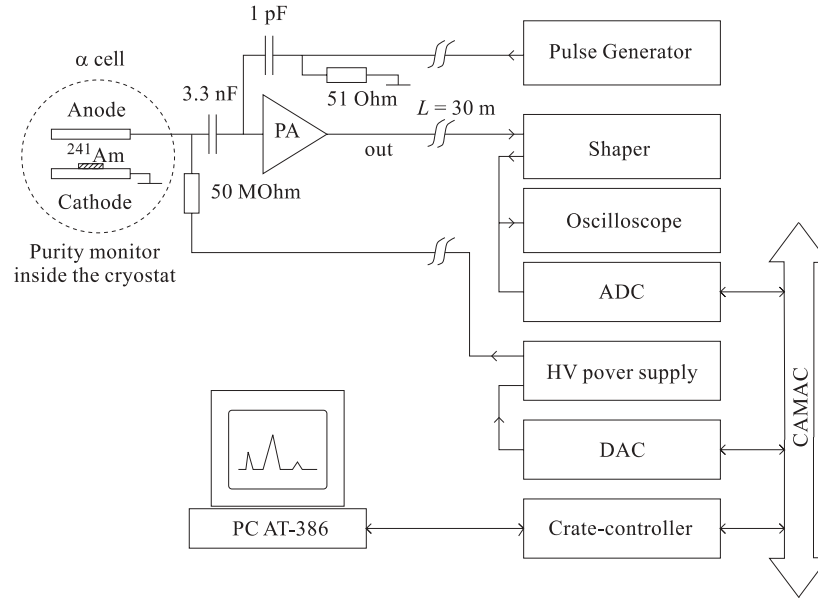


Fig. 2. The main readout scheme of the cold test facility

production in the liquid argon gap of 0.7 mm in between the anode and cathode. The output signal is amplified by a charge-sensitive preamplifier of RD-33 type (given by MPI, Munich). The preamplifier box contains a small board with the preamplifier chip and accompanying components and the HV-filter. For the period of measurements, it is mounted on the warm flange of the cryostat and connected to the anode via a  $100 \Omega$  cable 0.5 m long. The preamplifier has a feedback resistor  $R_f = 5.1 M\Omega$  and a capacitor  $C_f = 3.9$  pF. It is linked to the measurement equipment located in the counting room by coaxial cables 30 m long. The signal amplitude is about 5 V at the output of the amplifier system. High signal-to-noise ratio provides effective suppression of the pick-up signals in the collected charge spectra.

The amplified signal is fed through the attenuator into the shaper system [5] with a time constant chosen to be 200 ns. The amplitude spectra are recorded by 12-bit ADC (CAM.4.04-1 type produced by KFKI, Budapest) and stored on the disk of the personal computer. The rectangular calibration pulses (amplitude of  $0.2 \div 0.6$  V, 600  $\mu$ s period and width of 150  $\mu$ s), produced by the HP-8112A pulse generator, inject the test input of the preamplifier with the calibrated input capacitor  $C_0$ .

The procedure to calibrate the ADC scale in terms of collected charge value is presented in Fig. 3:

- Set of calibrated pulses from the interval of  $(1 \div 6)$  mV are recorded by the ADC (Fig. 3a). A Gaussian fit was applied to extract each peak position.
- Figure 3b shows the generated pulse amplitude (in mV) as a function of ADC counts. This figure demonstrates a good linearity over a wide range of ADC counts (the line represents the linear fit to the data). The ADC has a low intrinsic threshold and zero pedestal value.

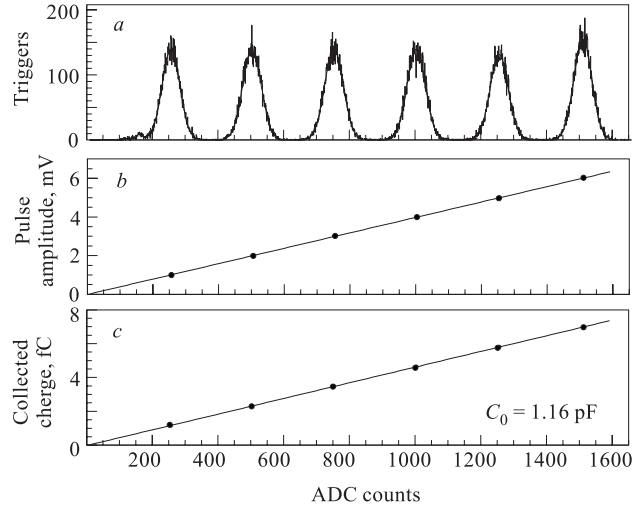


Fig. 3. Calibration of the ADC scale

- The calibration of the ADC scale is shown in Fig. 3c for the input capacitor  $C_0 = 1.16$  pF used in the experiment (it was changed later on to 1.05 pF). The same calibration constants were used for the data processing before and after each irradiation run.

**1.4. Neutron Rates.** Neutron fluence and kinetic energy spectrum of fast neutrons were measured in 1995 during the radiation hardness tests of the cold GaAs preamplifiers [6]. It was measured by means of the standard method of threshold detector activation. Since that time, some modifications to the reactor moderator were undertaken and the neutron flux became higher. Also, the collimator is foreseen in the present setup to focus the neutron beam on the argon vessel area to suppress the activation of the surrounding equipment.

The collimator made of blocks of polyethylene enriched of boron has a hole of dimensions  $10 \times 10$  cm<sup>2</sup> in front of the argon vessel. Its alignment was performed by means of  $\gamma$ -dosimeters fixed on the cryostat surface. The fast neutron spectrum was measured twice: without the collimator and behind it, on the cryostat surface. All spectra are compared in Fig. 4. It is seen that the collimator has suppressed the flux of fast neutrons by a factor 2, but the resulting spectrum is similar to the one measured in 1995.

The total fluence of fast neutrons is monitored by nickel dosimeters positioned around and inside the cryostat. The flux of fast neutrons ( $E_n > 100$  keV) in front of the cryostat was found to be  $(1.2 \pm 0.1) \cdot 10^{10}$  cm<sup>-2</sup>·s<sup>-1</sup>. Thus, during a campaign of reactor operation ( $\sim 250$  hours) a neutron fluence of about  $10^{16}$  cm<sup>-2</sup> could be achieved. The accuracy of the fluence measurement is about 10%. During the reactor operation a significant amount of  $\gamma$ 's are produced in the fission chains and in the reactions of neutron capture in surrounding materials. The  $\gamma$ -dose rate is about 400 Gy/h, giving an accumulated dose of about 100 kGy at the end of a standard 11 days run.

It was found during the test run that the neutron background produced by the neighbouring experiments was very high at the working position of the cryostat, resulting in thermal neutron activation of the argon. This activation does not provide reliable measurements of the  $\alpha$ -signal amplitude. This situation is responsible for some restrictions on the irradiation tests scenario.

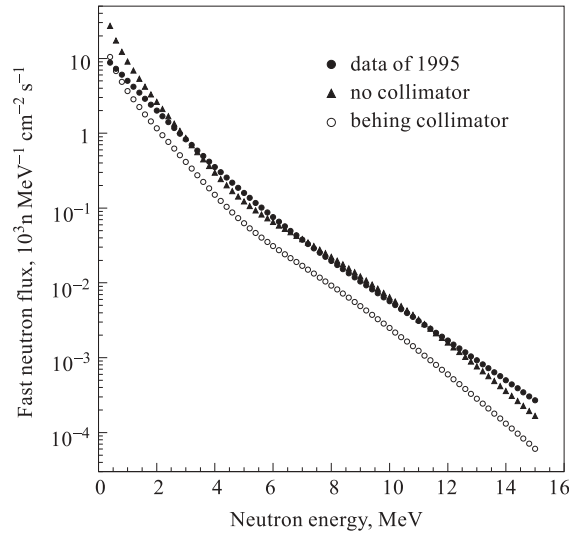


Fig. 4. Neutron energy spectra at IBR-2 reactor measured in front of the collimator and behind it on the cryostat surface. The spectrum measured in 1995 is represented by dots for comparison

In particular, the monitoring of the argon purity during irradiation is not possible. Also, when the irradiation run is finished, it is necessary to wait for a decrease of the induced activity of the argon, the tested materials, and the surrounding equipment. Both —  $\beta^-$  electrons (from  $n+^{40}\text{Ar}\rightarrow^{41}\text{Ar}\rightarrow^{41}\text{K}+\beta^-$ ) and electrons produced by Compton scattering of  $\gamma$  quanta, — affect the relevant signal. Activation of the equipment also causes some problems for access.

## 2. TEST MEASUREMENTS

The aim of the experiments is to study possible degradation of the  $\alpha$  signal caused by the irradiation of samples immersed in the liquid argon cryostat. For this purpose, the ADC spectra are recorded for various values of the high voltage in the range of (2÷29) kV/cm. Then, it becomes possible to determine the  $\alpha$ -peak position and to obtain the HV dependence of the charge value measured by the purity monitor. An example of ADC spectra is shown in Fig. 5, which represents the raw data collected at two different values of electric field in the liquid argon gap of the  $\alpha$  cell: 5.7 and 25.7 kV/cm.

Evidently, the amplitude of the  $\alpha$  signal is growing with the electric field, whereas the position of the reference peak used to monitor the gain of the preamplifier remains stable. The non-Gaussian tails of the  $\alpha$  peaks reveal the contribution of the pick-up signals.

A semiempirical model [7] could be used to extract the value of the impurity concentration (in ppm) in the case of the oxygen-polluted liquid argon. The ratio of two curves representing the collected charge, as a function of the electric field, measured after and before irradiation also provides relevant information (attenuation factor) about the signal loss due to the pollution of liquid argon.

**2.1. Analysis of Systematics.** The data processing is rather simple: *i*) the ADC spectrum has to be fitted by some functional to find the position of the  $\alpha$  peak, *ii*) the fitted position has

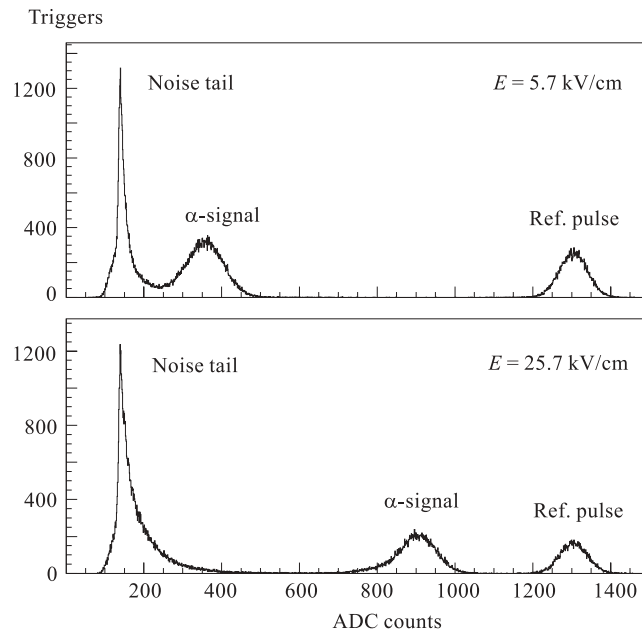


Fig. 5. An example of the raw data. Each histogram is an ADC spectrum containing 100 K triggers recorded for two different values of electric field in the liquid argon gap of the  $\alpha$  cell: 5.7 kV/cm and 25.7 kV/cm

to be corrected assuming the stability of the reference pulse, and finally, *iii*) the ADC counts must be translated into collected charge units (fC) for further analysis. Each step gives a certain contribution to the systematics which has to be summed with the statistical uncertainty taken from the (Gaussian) fit.

**Uncertainties due to the fit procedure** could be estimated from the variations of the peak position as determined from different fitting procedures. It is seen from Fig. 5 that at  $E = 5.7$  kV/cm the exponential tail of the noise peak, which is cut by the threshold, should be taken into account. The possible contribution of additional charge sources at higher E values could be described by additional Gaussians. On the other hand, each peak of the ADC spectra could be fitted by a single Gaussian in the  $\pm 1 \sigma$  interval around the peak position. Differences in results obtained from different fitting procedures are presented in Fig. 6,a. The variations are within the range of  $\pm 5$  ADC counts.

**The reference pulse position** was used to correct the gain of the preamplifier at each HV point. It is seen from Fig. 6,b that the reference peak position is varying during the measurements within the range of  $\pm 2$  ADC around the average value. This conclusion was checked to be valid over the whole ADC scale.

**Calibration of the ADC scale** in terms of fC was obtained from the linear fit of the calibration pulse positions. The fitted parameters were averaged over a set of measurements, and the deviations from this averaged calibration are presented in Fig. 6,c. Based on this calibration method, the uncertainty on the collected charge value is expected to be at the level of  $\sim \pm 0.01$  fC.

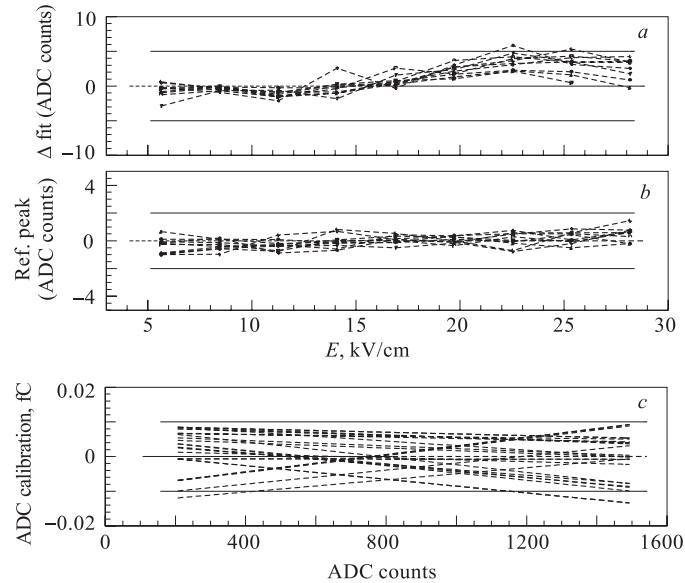


Fig. 6. Systematic errors estimated from different runs of measurements: a) uncertainty due to the fit procedure; b) variation of the reference signal around its average position; c) uncertainty on the ADC calibration

The detailed analysis of the systematic errors was performed for all irradiation runs, and no significant variation of the systematics was found from run to run.

**2.2. Sensitivity to the Oxygen Contamination.** The sensitivity of the Dubna preamplifier was tested at the Mainz facility [8] which is equipped with a precise laser chamber monitor allowing the accurate determination of the injected oxygen probe value. The output of the  $\alpha$  cell with similar gap size (0.8 mm) was measured by the Dubna preamplifier in parallel with the laser operation.

Data obtained at Mainz, shown in Fig. 7, demonstrate the ability of the preamplifier to recognize the liquid argon pollution at a level better than 1 ppm.

Some tests with oxygen probes were also performed at the Dubna facility with no beam from the reactor. The cryostat and connected tubes (of 8 mm diameter) were pumped out and the oxygen probe of known value was introduced into the cryostat. Then, the receiver filled with purified argon gas and positioned 10 m away from the cryostat was opened and the liquefaction process was started.

The procedure of probes injection gives some uncertainty on the oxygen concentration in liquid argon. There were three probes of oxygen used for the tests: (1.2 ÷ 1.9), (2.5 ÷ 3.9), and (3.8 ÷ 5.8) ppm. The smaller values in the parentheses correspond to the assumption that the oxygen probes are mixed uniformly inside the argon system (receiver, tubes, and cryostat). The larger values correspond to the probes liquefied completely inside the cryostat. The initial contamination can be expected to be close to the larger value because the liquefaction was over soon after the probe injection.

The signal losses observed in our tests with the oxygen polluted argon are presented in Fig. 8. The known dependence of the absorption factor with the contamination value  $\rho$  as the

only free parameter was fitted to the data:

$$Q_{\text{polluted}}/Q_{\text{pure}} = \lambda/d \times (1 - \exp(-d/\lambda))$$

with  $\lambda(\text{cm}) = 0.14 \times E(\text{kV/cm})/\rho(\text{ppm})$ , where  $d = 0.07 \text{ cm}$  is the  $\alpha$  cell gap size. The results of the fit are shown in Fig. 8. They are in agreement with the expected values noted in parentheses.

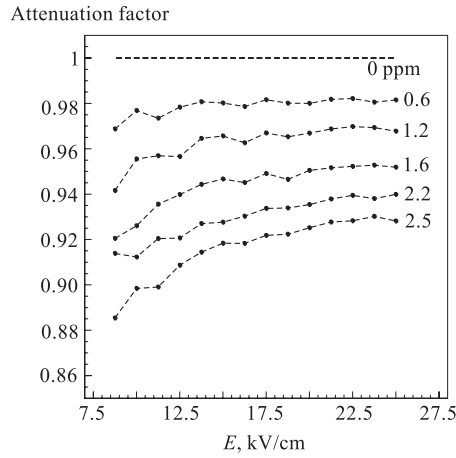


Fig. 7. Attenuation factor measured for low levels of oxygen impurities at the Mainz facility. The measurements have been carried out using the Dubna preamplifier

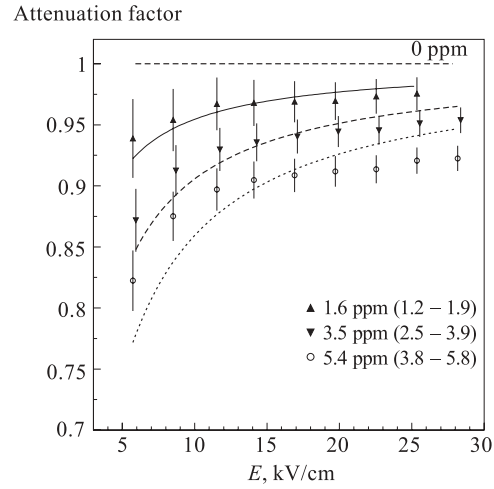


Fig. 8. Signal loss due to the oxygen impurities. The lines present the results of the fit. The values in parentheses indicate the range of the expected values of oxygen concentration

**2.3. Signal Stability.** The time dependence of the  $\alpha$  signal for the oxygen-polluted argon (at 5 ppm) is presented in Fig. 9.

The collected charge value is smaller by  $\sim 8\%$  compared to the value expected for the pure argon, because of the oxygen contamination. This is shown in Fig. 9,a where the dependence of the absorption factor on the electric field value is presented for four measurements performed with a time interval of about one day. The data in Fig. 9 are slightly shifted horizontally for clearer viewing.

The collected charge values measured 2 hours after liquefaction could be compared to the data obtained later on. The corresponding ratios of the charge values are plotted in Fig. 9,b. It is seen that the collected charge value became higher by  $\sim 2\%$ , i.e., liquid argon became cleaner in the cryostat. Collected charge is growing during the first day and then remains stable (see Fig. 9,c) as expected for the equilibrium state.

From Fig. 7, it could be observed that a signal loss of  $\sim 2\%$  corresponds to an oxygen contamination at the level of  $\sim 0.6 \text{ ppm}$ . The observed recovery of the monitor signal could smear signal attenuation caused by the small impurities (less than 1 ppm).

This «self-purification» effect is not induced by radiation damage but is caused by the absorption of the oxygen impurities on the inner surface of the liquid argon vessel and by

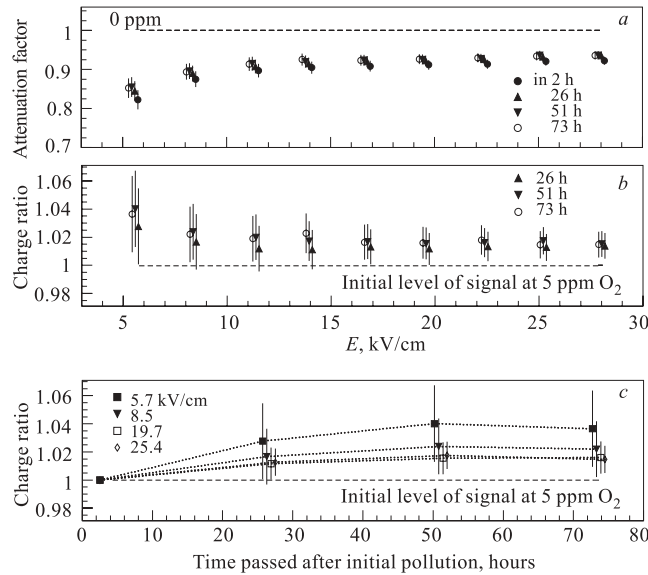


Fig. 9. Behaviour of the  $\alpha$ -cell signal with time for the oxygen polluted argon at 5 ppm: a) absorption factor measured in the period of three days (the dashed line indicates the expectation for pure argon) as a function of the electric field; b) ratio of the collected charge measured later on to the one measured soon after the liquefaction (the dashed line shows the initial measurements two hours after liquefaction); c) time dependence of the charge ratio for different values of the electric field. The data are shifted horizontally for clearer viewing

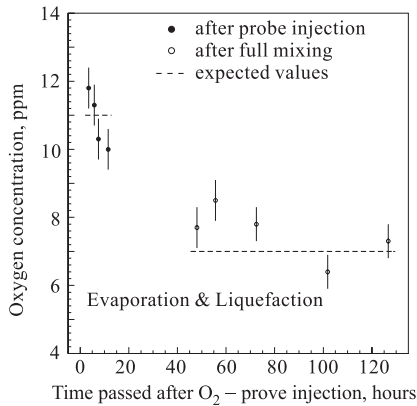


Fig. 10. Behaviour of the argon purity with time: soon after the oxygen probe injection (black dots) and during a long period after the full mixing of the oxygen probe and the argon gas (open dots). Dashed lines indicate the expected levels of the oxygen concentration, see text

the mixing of the oxygen polluted argon from the cryostat with initially purified argon gas contained in the receiver.

The hypothesis was checked in a special test with monitoring of intentional oxygen contamination of liquid argon in the cryostat over long period of time. About 6 cm<sup>3</sup> of oxygen gas were injected into the warm argon vessel of the cryostat which was pumped out beforehand for this test. The argon receiver with 850 l of argon gas was opened and 530 l of the argon were liquefied soon after in the argon vessel.

The maximal value of about 11 ppm concentration might be expected for the whole oxygen probe liquefied in the cryostat, and about 7 ppm — for the oxygen probe mixed uniformly in the liquid and gaseous states of argon in cryostat and receiver. The oxygen concentration values were determined by means of the model [7]. The results are presented in Fig. 10.

Argon purity becomes better with time after the initial liquefaction of the oxygen probe due to the mixing of the oxygen polluted argon in the cryostat and the argon gas in the receiver. The impurity level value is close to expectation. The «cleaning» could continue until the oxygen concentration in the argon system becomes even. The recurrent pressure variations in the argon vessel within  $(1.05 \div 1.10)$  bar results in the travel of  $\sim 15$  l of argon gas between the argon vessel and the receiver about ten times per hour. To speed up the process, the oxygen polluted liquid argon was evaporated from the cryostat back into the receiver and liquefied once more. The liquid argon was kept in the cryostat after this full mixing until the end of the test and the liquid argon purity remained stable within  $\pm 1$  ppm. It was found that variations of the monitor signal at the end of the test could be caused by the instability of the high voltage power supply. It will be replaced in the future runs.

### 3. RESULTS OF IRRADIATION COMPAGNS

**3.1. «Empty» Run.** The pollution tests for ATLAS have started in October 1998. First of all, the cryostat filled with liquid argon with no materials for test inside was exposed to a high dose (the so-called «EMPTY» run). The collected charge dependence on high voltage was measured twice — before and after the irradiation run (in two weeks). During the run the cryostat was exposed to a total fast neutron fluence of  $(1.0 \pm 0.1) \cdot 10^{16} \text{ cm}^{-2}$  and  $\gamma$  dose of  $(96 \pm 10)$  kGy. The results of the «EMPTY» run are presented in Fig. 11.

If the assumption is made that the liquid argon is polluted by oxygen, the model of Ref. 7 may be applied to estimate the impurity concentration before and after the irradiation run. Here, the model is used just to indicate the liquid argon pollution level and then, the extracted value of  $\rho$  (ppm) is not considered as the actual estimate of the concentration value. A careful calibration of the purity monitor (an  $\alpha$  cell) with the well-known level of the oxygen contamination is required in order to obtain model independent values of  $\text{O}_2$ -equivalent pollution. From [7], it has been found that  $\rho = (4.4 \pm 0.3)$  ppm and  $(3.7 \pm 0.2)$  ppm before and after the irradiation, respectively. A nonzero value of the initial liquid argon purity concentration was caused by lack of time for a careful cleaning of the 300 litres receiver after its preparation (it takes about 20 hours to fill it with pure argon). This was not the case for the subsequent runs since the system was, then, cleaned up by multiple flushing with pure argon gas.

The liquid argon purity before and after the irradiation run are similar. So, the cryostat itself does not pollute argon during irradiation.

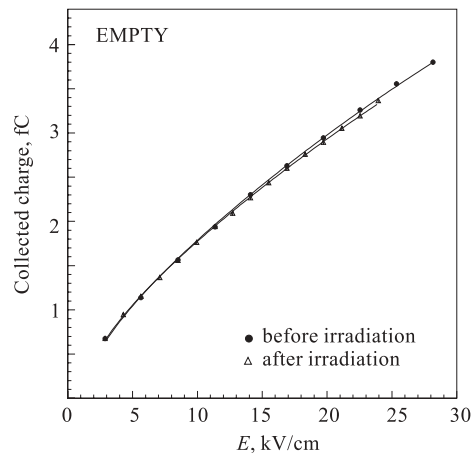


Fig. 11. Results of an «EMPTY» irradiation run with no materials for test in the cryostat. The collected charge dependence on the electric field was measured before and after irradiation up to the neutron fluence of  $10^{16} \text{ cm}^{-2}$

**3.2. Irradiation of PEEK Fibres.** The PEEK fibres were tested with respect to their possible outgassing under irradiation and the possible pollution of liquid argon during the next irradiation run undertaken in November 1998. Since the October run, a new readout electronics has been developed to operate with a much wider ADC scale. The fibres of 0.375 mm in diameter and 750 m of total length were positioned inside the cryostat. About 0.9 litres of liquid argon was liquified in the argon vessel. The samples were irradiated up to the total neutron fluence of  $(1.0 \pm 0.1) \cdot 10^{16} \text{ cm}^{-2}$  and  $\gamma$  dose of  $(96 \pm 10) \text{ kGy}$ .

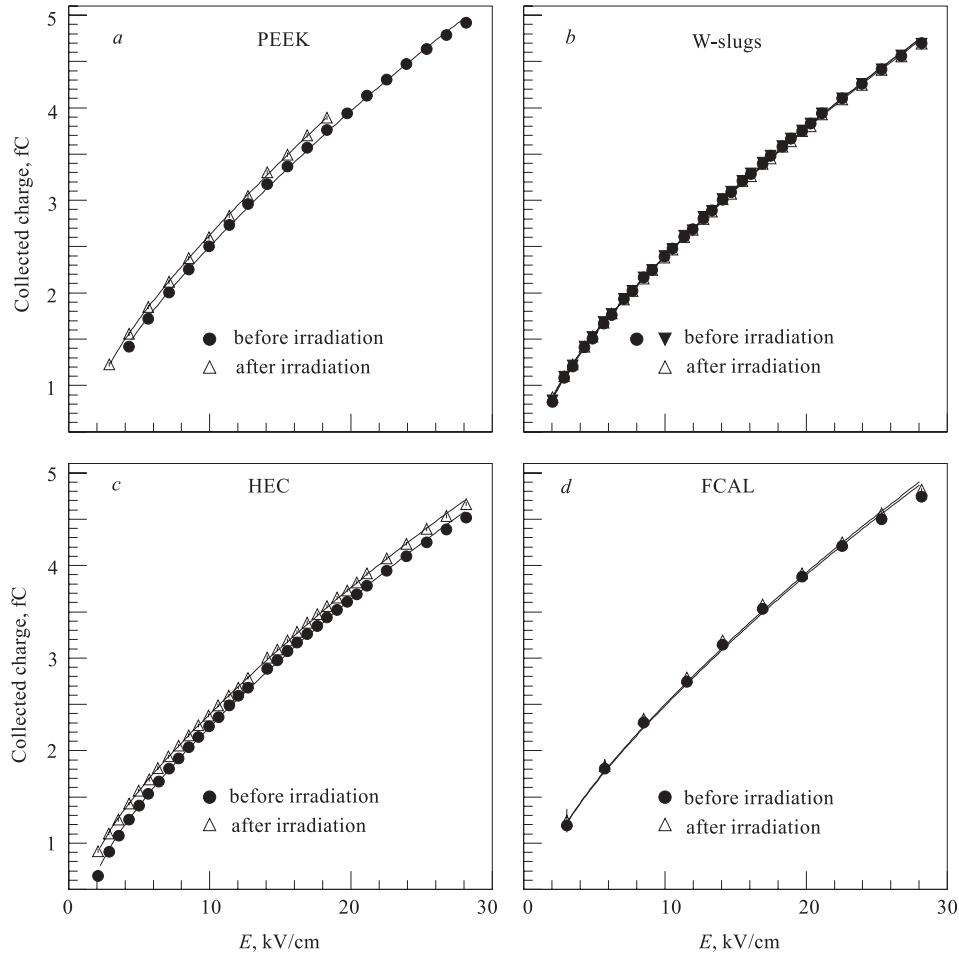


Fig. 12. Summary of the irradiation campaigns. The collected charge was measured before and after irradiation up to the typical value of the neutron fluence of  $10^{16} \text{ cm}^{-2}$ . The results are presented for four runs: a) PEEK run, b) W-slugs run, c) HEC run and d) FCAL run

The summary of the «PEEK» run is shown in Fig. 12,a. Based on the model [7], one may estimate the «oxygen» contamination before and after the irradiation at the level of  $(0.7 \pm 0.2) \text{ ppm}$  and  $(0.2 \pm 0.2) \text{ ppm}$ , respectively.

The initial value of 0.7 ppm is lower than the value measured in the «EMPTY run» because of a better cleaning of the argon system. Unfortunately, this time an argon leak into the vacuum vessel of the cryostat prevented the measurement of the collected charge over the whole high voltage range.

Nevertheless, the comparison of the collected charges and impurities concentration values obtained before and after the irradiation gives no indication of liquid argon poisoning due to radiation damage of the PEEK fibres.

**3.3. Irradiation of Tungsten Slugs.** The December 1998 run of the IBR-2 reactor was carried out to test the tungsten sintered slugs stability under irradiation. The total volume of the samples immersed in 0.6 litre of liquid argon was 231 cm<sup>3</sup>. The cryostat was exposed to the neutron fluence of  $(1.0 \pm 0.1) \cdot 10^{16}$  cm<sup>-2</sup> and  $\gamma$  dose of  $(107 \pm 11)$  kGy. Results of the «W-slugs» run are presented in Fig. 12,*b*. The collected charge measured as a function of the electric field before the irradiation run with a time interval of one day is compared to the collected charge dependence on the electric field after the shutdown of the IBR-2 reactor.

The impurity level estimates are  $(0.6 \pm 0.1)$  ppm and  $(0.5 \pm 0.1)$  ppm before the reactor run and  $(0.3 \pm 0.1)$  ppm after the irradiation. It is seen that the concentration values are similar for the three measurements considered. Thus, high radiation dose absorbed by the tungsten slugs did not induce pollution of liquid argon. This result is in agreement with the measurements of outgassing which were carried out earlier at Arisona [9] and at Dubna [10].

**3.4. Irradiation of HEC Materials.** A set of different materials used in the liquid argon gap of the hadronic end-cap (HEC) calorimeter was collected for a pollution test in January 1999. The combination of materials represented one half of the HEC liquid argon gap. Finally, two honeycomb sheets, one EST board, one half of the PAD and PSB boards, fasteners, different connectors, striplines, and cables were immersed in the cryostat filled with 0.6 litres of liquid argon.

The total fluence of fast neutrons achieved was  $(1.3 \pm 0.2) \cdot 10^{16}$  cm<sup>-2</sup> and  $\gamma$  dose of  $(107 \pm 11)$  kGy. A summary of the measurements is presented in Fig. 12,*c*. It is seen that the value of the collected charge measured after irradiation is always higher compared to the value measured before irradiation. This means that the liquid argon becomes cleaner. It would be necessary to flush and pump out the cryostat during a long period of time before the run to eliminate the initial contamination caused by the outgassing from the tested samples (honeycomb materials, namely, could absorb a large amount of water during their transportation). As it was done for the previous runs, one may obtain an indication of the argon purity after irradiation. The impurity concentration before and after the irradiation was estimated to be  $(1.7 \pm 0.1)$  ppm and  $(0.03 \pm 0.08)$  ppm, respectively.

Thus, no pollution due to the irradiation of the HEC materials has been found after a neutron fluence of  $1.3 \cdot 10^{16}$  cm<sup>-2</sup>.

**3.5. Irradiation of FCAL Materials.** Two types of the interconnectors, kapton cables, and samples of electrodes were used for the pollution tests in April 1999. The total length of polyimide cables placed in the cryostat was about 30 m. There were also 173 glueless copper-clad polyimide interconnectors and 9 samples of electrodes (later the electrodes were tested for peeling [11]) immersed in 0.7 litre of liquid argon.

The shutdown of the IBR-2 reactor happened three days before the official date, and therefore the materials were exposed up to a total fluence of  $(0.7 \pm 0.1) \cdot 10^{16}$  cm<sup>-2</sup> and  $\gamma$  dose of  $(67 \pm 7)$  kGy. The results of the collected charge measurements before and after the irradiation are shown in Fig. 12,*d*.

The estimate of the impurity concentration obtained before and after the irradiation is found to be  $\sim 0$  ppm, for both measurements. Thus, no pollution due to the irradiation of the FCAL interconnectors and cables was found after the neutron fluence of  $0.7 \cdot 10^{16} \text{ cm}^{-2}$ .

#### 4. DISCUSSION

In Fig. 13, the ratios of the collected charge measured after and before the irradiation as a function of the electric field are presented for all the runs carried out at the IBR-2 reactor during the period October 1998–April 1999.

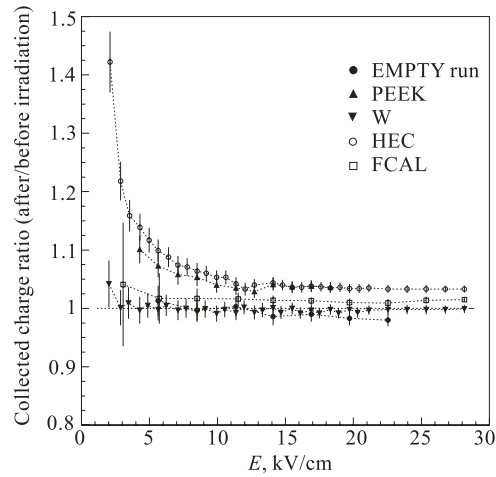


Fig. 13. Ratio of the collected charge values measured after and before the irradiation in five campaigns as a function of the electric field

If the irradiation of materials immersed in the cryostat would cause the pollution of liquid argon, one could observe degradation of the collected charge value, and the charge ratio measured after and before the irradiation (attenuation factor) would be less than unity. In our experiments, this charge ratio is close to unity for all the tested materials.

The higher values of the ratio in the HEC run could be explained as the consequence of absorption of the impurities in large amount of the friable honeycomb samples during the two weeks period of irradiation and by the mixing of impurities with pure argon in the argon gas receiver (see Fig. 9,b). Initial degradation of the signal due to outgassing was already seen before that test.

#### 5. CONCLUSIONS

The basic developments of the cold test facility at IBR-2 reactor in Dubna were completed in 1998. Five irradiation runs were carried out to test the pollution of liquid argon possibly caused by radiation damage. The cryostat containing the samples to be tested was exposed typically to a high total neutron fluence of  $10^{16} \text{ cm}^{-2}$  and a  $\gamma$  dose of  $\sim 100 \text{ kGy}$ .

Irradiation of an empty cryostat (with no materials immersed in liquid argon) has demonstrated that the argon system of the facility withstands high radiation doses and does not pollute liquid argon.

The FCAL materials — PEEK fibres, tungsten slugs, interconnectors, kapton cables, and samples of electrodes — were tested in three runs and no indication of argon pollution caused by irradiation has been found.

The same conclusion could be drawn from the irradiation of the HEC materials representing one half of the liquid argon gap of the calorimeter.

**Acknowledgements.** The authors wish to thank J. Collot and Ph. Martin from ISN, Grenoble, for stimulating and fruitful discussions. Financial support from NSERC/Canada and ATLAS Collaboration is gratefully acknowledged. We are pleased to mention hospitality and assistance of our colleagues K. Jakobs and C. Zeitnitz from University of Mainz.

### References

1. Cheplakov et. al. A. — Nucl. Instr. and Meth., 1998, v.A411, p.330.
2. Ichimura K., Ashida K., Watanabe K. — J. Vac. Sci. Technol., 1981, v.18, p.1117.
3. Rivkis L.A. et al. — Protocol of tests, Bochvar Institute, Moscow, 1997 (unpublished).
4. Golovanov L.B. et al. — Nucl. Instr. and Meth., 1996, v.A381, p.15.
5. de la Taille C. — Orsay Preprint, LAL/RT 92-10 (1992).
6. Cheplakov et al. A. — JINR Preprint P13-96-403, Dubna, 1996; Nucl. Instr. and Meth. A (to be published).
7. Andrieux M.L. et al. — Nucl. Instr. and Meth., 1999, v.A427, p.568.
8. Adams M. et al. — ATLAS Note, ATL-LARG-96-053, 26 November 1996.
9. Rutherford J., Savin A., Shaver L. — ATLAS Note, ATL-LARG-99-007, 6 January 1999.
10. Leroy C. et al. — ATLAS Note, ATL-LARG-99-020, 25 October 1999.
11. Leroy C. et al. — ATLAS Note, ATL-LARG-99-018, 14 October 1999.

Received on July 27, 2000.